STScI | SPACE TELESCOPE SCIENCE INSTITUTE

Instrument Science Report WFC3 2021-06

WFC3/UVIS: New FLC External CTE Monitoring 2009 - 2020

Benjamin Kuhn & Jay Anderson

June 11, 2021

Abstract

With the recent release of a new pixel-based CTE-correction (v2.0) in the `calwf3` *(v3.6.0) calibration pipeline, we present updates to the Charge Transfer Efficiency (CTE) residual flux losses measured in the WFC3/UVIS External CTE programs (2009-2020). Using observations of 47 Tuc (NGC 104) and NGC 6791 we analyze the flux loss of stars due to diminishing CTE by comparing relative aperture photometry of a given source at varying distances from the readout amplifiers on a variety of image background levels. A photometric correction model that depends on source flux, observation date, and the source distance from the readout amplifiers was fit to the data for each background level. The coefficients derived from fitting the model to the data are provided for observers to (further) correct point-source photometry in new* `calwf3` *(v3.6.0)* `flc.fits` *files. We show through the residual CTE flux losses after the application of either the v1.0 or v2.0 CTE-correction that neither model works perfectly. The v2.0 correction often under-corrects photometry, while the v1.0 correction often over-corrects. The v1.0 correction works best at a background of 12 e^-, where the faintest sources measured (250-500 e^- within a 3-pixel radius aperture furthest from the readout) are over-corrected by ∼5% in 2020. At higher backgrounds, the over-correction is larger. The new v2.0 model does its best job at a background of 20 e^-, where the faintest sources measured (furthest from the readout amplifier) are under-corrected by ∼17% in 2020. The best pre-observation CTE mitigation strategy still remains to minimize losses in the first place, by placing the target near the readout amplifier (when possible) and post-flashing to ensure adequate total background (sky+dark+post-flash). As of April 2021, all* `flc` *and* `drc` *products retrieved from MAST will use the v2.0 correction, but users have the option of calibrating UVIS data with the v1.0 correction following the instructions in a recently published Jupyter-Notebook.*

1 Introduction

The UVIS channel in WFC3 contains two butted 4096 × 2051 CCD detectors that provide imaging in the UV to visible wavelengths (200 - 1000 nm). CCDs are complex but advantageous electronic detectors often used for astronomical observations. One of the procedures that occur during a CCD exposure is the readout process. This is when the collected clouds of electrons transfer from one pixel to the next and ultimately to the readout amplifier. The action of transferring the charge between pixels is imperfect for CCDs and it is important to measure the efficacy of the transfer.

This measurement is known as Charge Transfer Efficiency (CTE) and has been degrading ever since WFC3 reached above the shielding atmosphere of Earth when it was installed on-board HST. The decline in CTE is mainly due to the energetic particles present in HST's low-Earth orbital environment that damage the atoms in the detector's crystal silicon lattice. The pixels that have defects can temporarily trap fractions of the charge packet passing through it and subsequently release that change in a random process on timescales from microseconds to seconds (Baggett et al. 2011). This results in trails of misplaced charge in the image, with pixels furthest from the amplifier (closest to the chip gap) being affected the most. CTE depends on multiple scene characteristics such as the distance (in pixels) from readout, signal level, total background level, and the amount of sustained radiation damage.

The CTE flux loss of point sources in the UVIS detector is monitored via the external CTE calibration program. This program takes image-pairs of star clusters with a vertical one-chip dither between the two exposures. Making a relative comparison of the flux for a given source at varying distances from the readout amplifiers allows us to measure the loss in flux due to degrading CTE. Sources are grouped by their flux within a 3-pixel radius aperture and the CTE flux losses are analyzed as a function of the $\log_{10}$ of the flux bin as well as a function of observation date. Results from the external CTE program were first published by Kozhurina-Platais et al. (2011) and most recently by Kuhn and Bajaj (2021). For a synopsis of previous external CTE results, overall description of the data and observing strategy see Kuhn and Bajaj (2021) and references therein.

One of the available mitigation techniques used to minimize flux loss due to poor CTE makes use of an empirical pixel-based correction that restores charge to its original pixel (Anderson and Bedin 2010). This post-observation correction was first created for the Advanced Camera for Surveys (ACS) and delivered to the `CALACS` pipeline in Spring of 2012. While WFC3 had only spent about three years on-board HST in 2012, CTE losses were already substantial (50% or more when the background is low, suspected to be due to an increased rate of radiation damage sustained during the solar minimum) so the model was adapted for UVIS. In 2013, a standalone FORTRAN program became available for use, and between 2016-2021 observers could retrieve WFC3 v1.0 CTE-corrected data (level-2 product `flc.fits`) directly from the Mikulski Archive for Space Telescopes (MAST[1]).

Since 2017 the development of a new CTE-correction model has been underway through various WFC3/UVIS calibration programs (14531, 14534, 14880, 16440, 16029, 16441). In

[1]https://archive.stsci.edu/

late 2020 the new v2.0 pixel-based CTE-correction model was completed and, after thorough testing, released in the `calwf3` calibration pipeline in late April of 2021 (`calwf3` Version 3.6.0). A new Instrument Science Report from Anderson et al. (2021) (in prep) provides a detailed discussion of the new model (with comparison to the old model), the implications of the new correction, as well as pre and post-observation recommendations. With the deployment of a new model, observers will be interested to know the change in external CTE residual flux losses between the two models. In this report we have reprocessed the 2009-2020 external CTE data through `calwf3` with the new v2.0 2021 pixel-based correction and present a comparison in CTE flux loss between the versions. The UVIS external CTE results culminate in updated model coefficients to be used with the photometric correction formula in order to further correct point-source photometry in new v2.0 CTE-corrected `flc.fits` images. Throughout the remainder of this report we will use the v2.0 nomenclature to refer to the new pixel-based CTE-correction that is applied to `flc.fits` products in calwf3 versions 3.6.0 and beyond.

2 Data

UVIS external CTE data were routinely acquired through the calibration programs listed in Table 1. For each program, short (30 and 60 seconds) and long (348 and 420 seconds) exposures are taken in F502N. In November of 2012, (program 13083) we began to simulate various background levels via the post-flash method.[2] With the varying exposure times and post-flash levels, the total background levels explored in the external CTE monitor range from ∼0.1-0.5 e^- to ∼117-119 e^-. See Kuhn and Bajaj (2021) for a more in depth discussion about the data and observing strategy.

3 Results

Our calibration and analysis followed the same procedures as those described in Kuhn and Bajaj (2021), which used the methodology and observing strategy as all previous UVIS external CTE studies. The only difference is that in this report we have processed the data with `calwf3 v3.6.0`, which contains the new v2.0 CTE-correction. We have have separated our results based on the background level with two main figures each. The first type of figure illustrates CTE flux loss as a function of $\log_{10}$ of the flux, in a background-subtracted 3-pixel radius aperture, with model fits[3] over-plotted. Each of these plots have a color-bar associated with it that represent the epoch of the observation. The second set of figures show the evolution of CTE flux loss as a function of observation date for three main flux bins: 500-2000, 2000-8000, and 8000-320000 e^-. All of the figures have three panels that represent the CTE flux losses in (left to right) `flt.fits`[4], v1.0 `flc.fits`, and v2.0 `flc.fits`

[2]Prior to 2020, it was recommended that observers post-flash to a total background level of 12 e^- to help improve CTE. As of June 2020, the new recommended total background (dark+sky+post-flash) is 20 e^-.

[3]These fits are from the bivariate photometric correction model, which is completely separate from the pixel-based CTE-correction in `calwf3`

[4]`flt.fits` images are those which have been processed through `calwf3` without the pixel-based CTE-correction.

Table 1: UVIS external CTE monitor observations

Program ID	Principal Investigator	Observation Epochs (MM/YYYY)
11924	Kozhurina-Platais	10/2009, 03/2010, 09/2010
12348	Baggett	09/2010
12379	Noeske	11/2010, 03/2011
12692	Noeske	10/2011, 03/2012, 07/2012
13083	Noeske	11/2012, 03/2013, 07/2013, 08/2013
13566	Noeske	01/2014, 07/2014
14012	Gosmeyer	01/2015, 02/2015, 07/2015
14378	Mack	01/2016, 07/2016, 08/2016
14541	Mack	01/2017, 07/2017
14990	Fowler	01/2018, 07/2018
15576	Kurtz	02/2019, 07/2019
15721	Khandrika	01/2020, 06/2020, 07/2020

images. In addition to the figures, Table 4 - 6 lists the polynomial coefficients derived from fitting the photometric correction formula to the new v2.0 CTE-corrected (`flc`) data. These tables have been placed in the Appendix section below a short description of the empirical photometric correction.

Figures 1 and 2 represent the worst-case scenario for CTE due to the low background level ($\sim$0.1-0.5 e^-) and short exposure time. Under these conditions, the faintest sources (250-500 e^- within a 3-pixel radius aperture) processed with the v2.0 CTE-correction show a $\sim$30% residual flux loss in 2020 while the sources in the brightest flux bin (20000-32000 e^-) show a $\sim$2% residual flux loss, compared to 45% and 5% flux loss in the old 2016 CTE-corrected data. In the long exposure images with no post-flash (background of $\sim$1-3 e^-) processed with the new v2.0 CTE-correction, the faintest sources are under-corrected by $\sim$7% and the brightest sources show only a $\sim$0.3% under-correction in 2020, compared to 11% under-correction and a $< 1\%$ over-correction in the old v1.0 CTE-corrected `flc`s.

The results in Figure 3 characterize the CTE residual flux losses for short exposure data with a 12 e^- post-flash (backgrounds of $\sim$12.1-12.5 e^-). The losses in these plots begin to depict some of the most dramatic improvements between the old v1.0 `flc`s and the new v2.0 `flc`s (middle and right panels respectively). The old v1.0 pixel-based CTE-correction, in `calwf3` versions 3.3 - 3.5.2, over-corrected most data by a few percent; especially the low-moderate flux sources. The new 2021 pixel-based CTE-correction, in `calwf3` version 3.6.0 (and beyond), no longer over-corrects the low-moderate flux sources and the few available high flux sources are over-corrected by $< 1\%$ in 2020. The right panel of Figure 3 shows that the faintest sources processed with the v2.0 CTE-correction are under-corrected by $\sim$19% in 2020, compared to a $\sim$2% over-correction in the old v1.0 CTE-corrected `flc`s.

The CTE residual flux loss for the low-moderately bright sources processed with the v2.0 CTE-correction (∼2.5-3.75 on the x-axis) have improved by no longer being over-corrected, but the brighter sources (>3.75 on the x-axis) may still be slightly over-corrected (< 1%). However, as the error-bars illustrate, these measurements are less trustworthy due to the low number of stars in the flux bins. The 2020 data has between three and nine stars in the flux bins > 4000 e^-, while the flux bins < 4000 e^- have between 26 and 375 stars.

Figure 5 illustrates the CTE flux loss results for long exposure data with a background of ∼13-15 e^- (12 e^- post-flash). This is the nominal background level that the WFC3 team recommended observers obtain between 2012-2020 to help pre-fill charge traps and mitigate CTE losses. Sources with a flux of 250-500 e^-, furthest from the amplifier and processed with the new v2.0 CTE-correction, now show a ∼17% under-correction in 2020, compared to an 8% over-correction in the old v1.0 CTE-corrected data. The sources with a flux of 20000-32000 e^- are slightly over-corrected by ∼0.2% in 2020, compared to a 1% over-correction in the old v1.0 CTE-corrected `flc`s.

In June of 2020, the WFC3 team changed the total background recommendation from 12 to 20 e^- due to degradation of the CTE from further (expected) radiation damage. Figure 7 shows the CTE flux losses for data with a ∼19-21 e^- background. Using the old v1.0 CTE-correction, the faintest sources measured experienced an over-correction by ∼13% in 2020. In the new v2.0 correction, these same sources are no longer over-corrected and in 2020 have a CTE flux loss of ∼17% (furthest from the amplifier). With a ∼19-21 e^- background, the brightest sources are over-corrected by ∼0.1% in 2020 using the new CTE-corrected `flc`s. This is an improvement from the old v1.0 CTE-corrected `flc`s where the brightest sources were over-corrected by ∼1%.

In an effort to summarize some of the results displayed in the figures of CTE flux loss evolution (such as Figure 2), we have created Tables 2 and 3. These two tables list the percentage of CTE flux loss in the 2020 data as well as the overall CTE loss evolution (in units of Δmag/2051 pix/yr) using the v2.0 `flc` files. Furthermore, while we have only highlighted four background levels, figures have been uploaded to the WFC3 CTE resource page that exhibit the CTE flux loss and evolution for the remaining background levels.

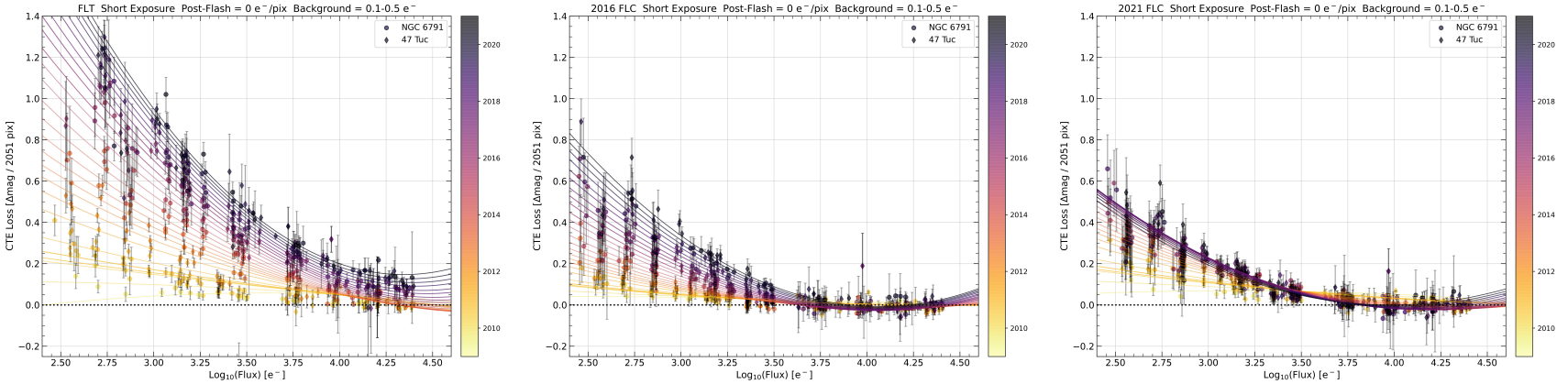

Figure 1: CTE flux losses as a function of $\log_{10}$ of the flux within a 3-pixel radius aperture for FLT, 2016 `flc`, and new 2021 `flc` short exposure data with a ∼0.1-0.5 e^- total background level (0 post-flash, furthest from the readout). The circles represent NGC 6791 data and the diamonds represent 47 Tuc data. The color bar on each plot corresponds to the epoch of the observation in units of decimal year.

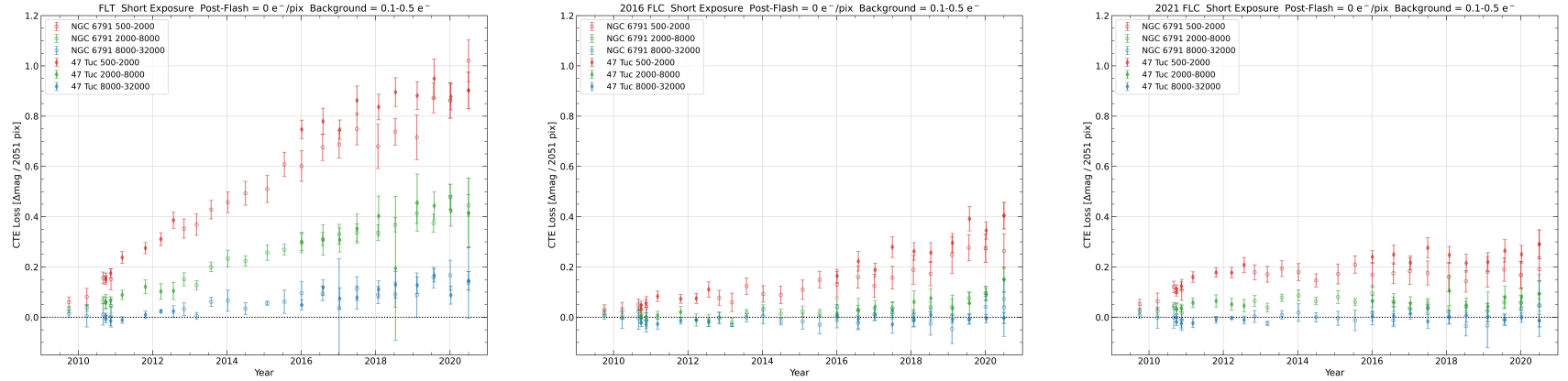

Figure 2: CTE flux losses as a function of observation date for FLT, 2016 `flc`, and new 2021 `flc` short exposure data with a ∼0.1-0.5 e^- total background level (0 post-flash, furthest from the readout). The circles represent NGC 6791 data, the diamonds represent 47 Tuc data, and the values in the legend correspond to three of the flux bins, in units of e^- (within a 3-pixel radius aperture), which cover approximately the entire range of fluxes measured.

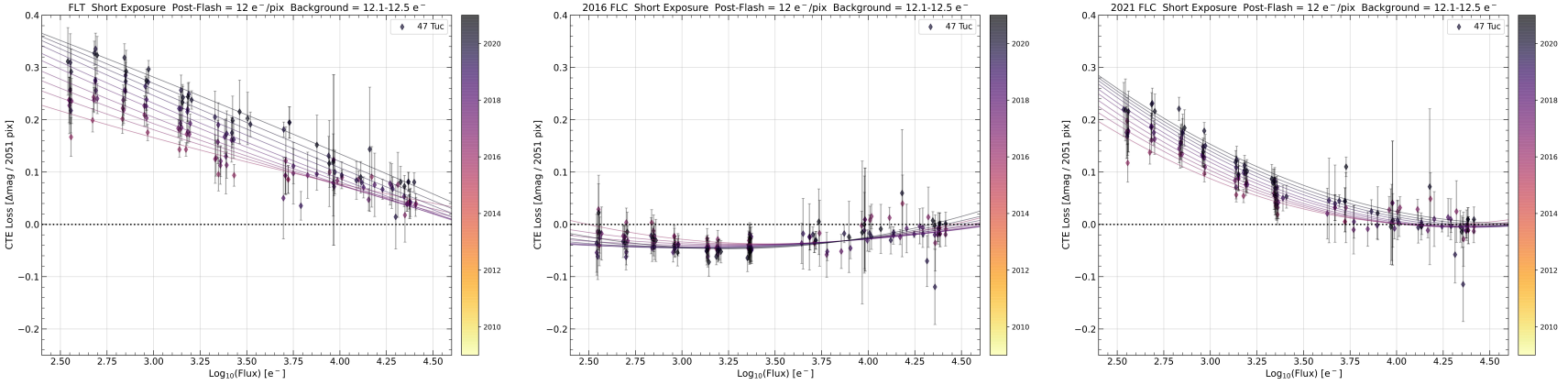

Figure 3: CTE flux losses as a function of $\log_{10}$ of the flux within a 3-pixel radius aperture for FLT, 2016 `flc`, and new 2021 `flc` short exposure data with a ∼12.1-12.5 e$^-$ total background level (12 e$^-$ post-flash, furthest from the readout). The color bar on each plot corresponds to the epoch of the observation in units of decimal year.

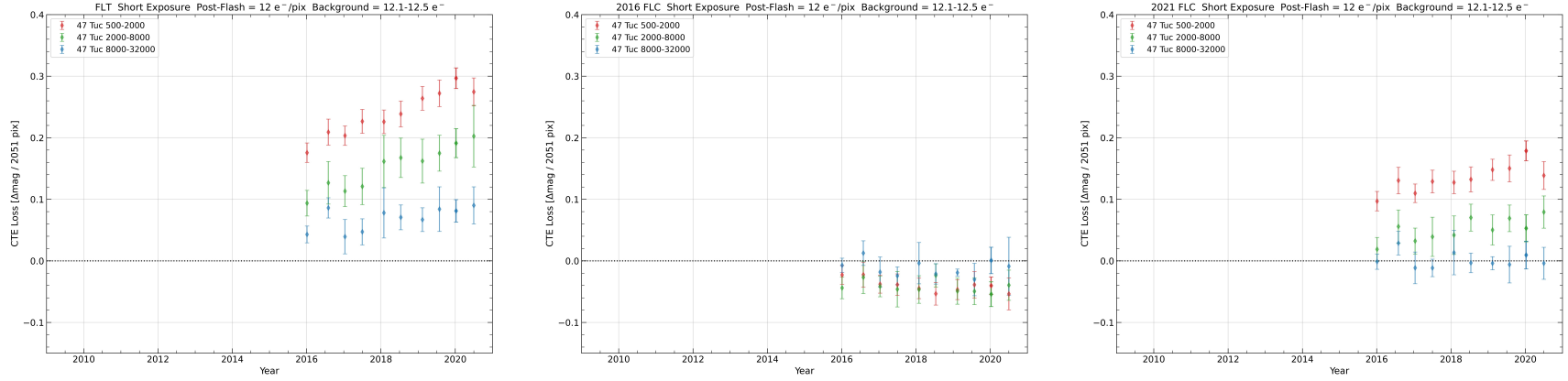

Figure 4: CTE flux losses as a function observation date for FLT, 2016 `flc`, and new 2021 `flc` short exposure data with a ∼12.1-12.5 e$^-$ total background level (12 e$^-$ post-flash, furthest from the readout). The values in the legend correspond to three of the flux bins, in units of e$^-$ (within a 3-pixel radius aperture), which cover approximately the entire range of fluxes measured.

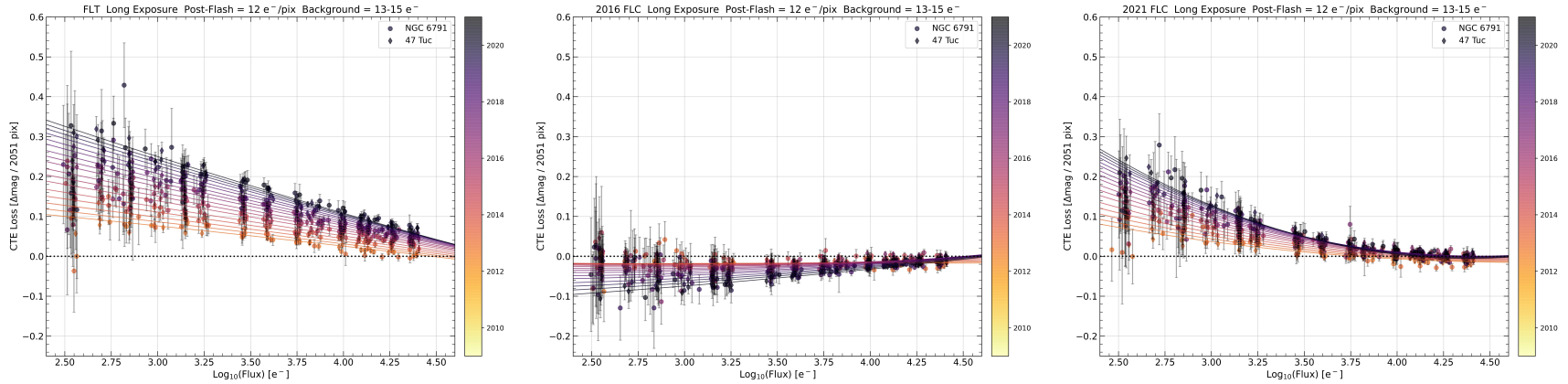

Figure 5: CTE flux losses as a function of $\log_{10}$ of the flux within a 3-pixel radius aperture for FLT, 2016 `flc`, and new 2021 `flc` long exposure data with a ∼13-15 e^- total background level (12 e^- post-flash, furthest from the readout). The circles represent NGC 6791 data and the diamonds represent 47 Tuc data. The color bar on each plot corresponds to the epoch of the observation in units of decimal year.

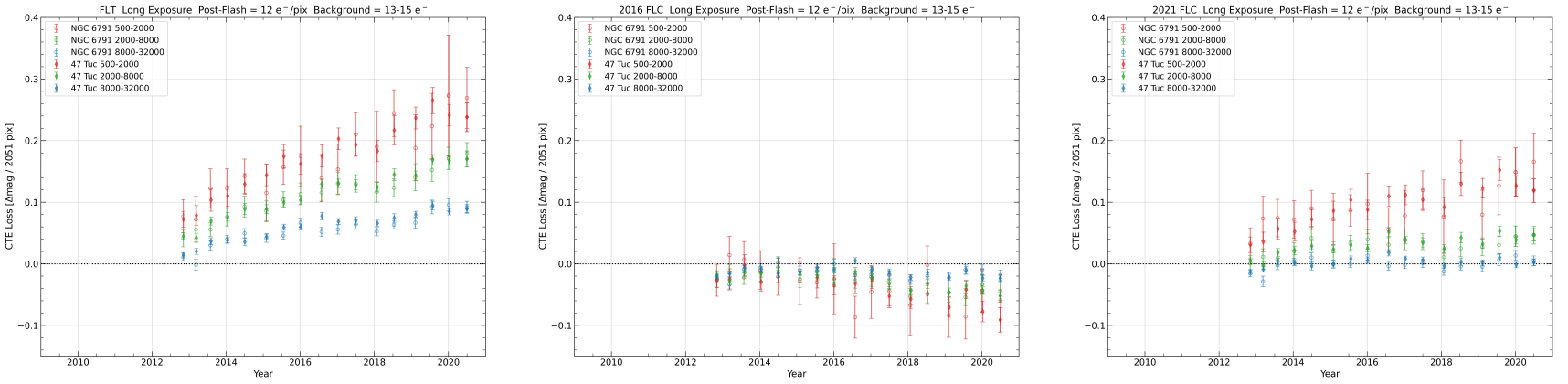

Figure 6: CTE flux losses as a function of observation date for FLT, 2016 `flc`, and new 2021 `flc` long exposure data with a ∼13-15 e^- total background level (12 e^- post-flash, furthest from the readout). The circles represent NGC 6791 data and the diamonds represent 47 Tuc data. The values in the legend correspond to three of the flux bins, in units of e^- (within a 3-pixel radius aperture), which cover approximately the entire range of fluxes measured.

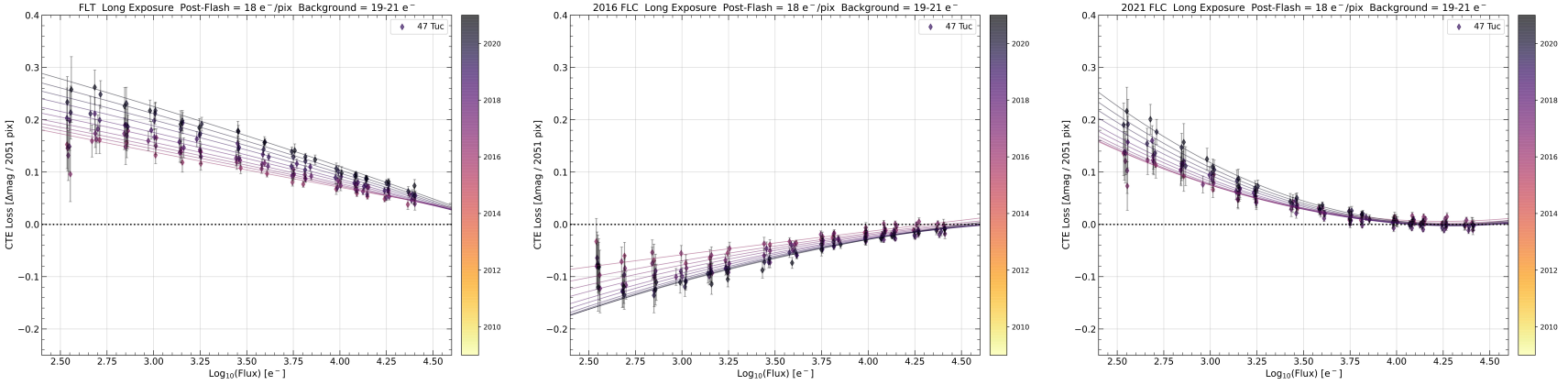

Figure 7: CTE flux losses as a function of $\log_{10}$ of the flux within a 3-pixel radius aperture for FLT, 2016 `flc`, and new 2021 `flc` long exposure data with a ∼19-21 e$^-$ total background level (18 e$^-$ post-flash, furthest from the readout). The color bar on each plot corresponds to the epoch of the observation in units of decimal year.

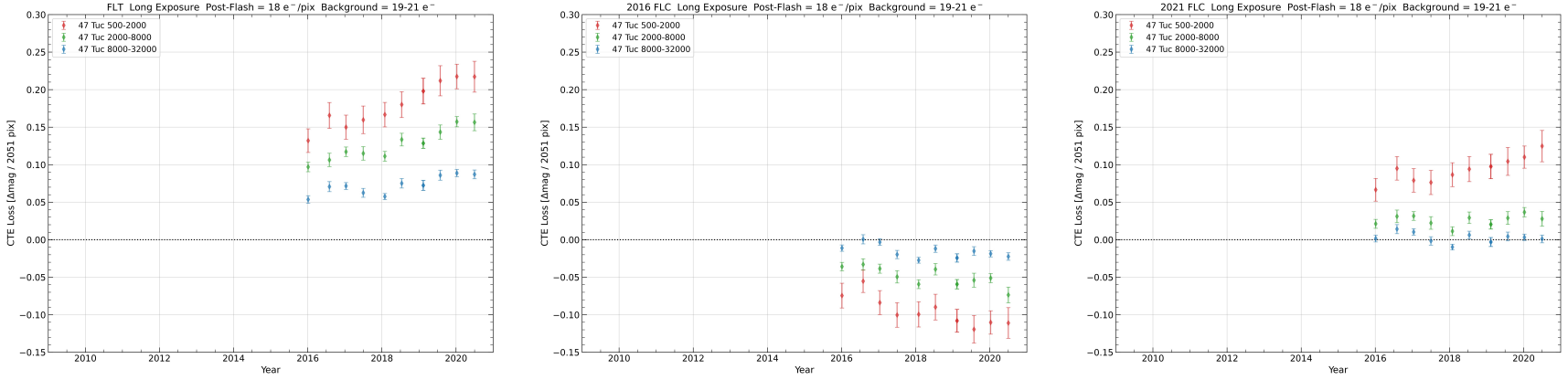

Figure 8: CTE flux losses as a function of observation date for FLT, 2016 `flc`, and new 2021 `flc` long exposure data with a ∼19-21 e$^-$ total background level (18 e$^-$ post-flash, furthest from the readout). The values in the legend correspond to three of the flux bins, in units of e$^-$ (within a 3-pixel radius aperture), which cover approximately the entire range of fluxes measured.

Table 2: CTE Flux Loss Evolution and Percent Flux Loss for New v2.0 `FLC` Data

Background [e$^-$]	0.1-0.5		1-2		7-9		12-12.5	
Flux Bin [e$^-$]	CTE loss rate^i	CTE flux loss^{ii}	CTE loss rate^i	CTE flux loss^{ii}	CTE loss rate^i	CTE flux loss^{ii}	CTE loss rate^i	CTE flux loss^{ii}
500-2000	0.01	19%	0.0009	8%	0.01	15%	0.01	14%
2000-8000	0.003	6%	0.004	5%	0.006	6%	0.009	7%
8000-32000	0.002	1%	0.002	1%	0.001	0.7%	-0.001	0.2%

[i] Δmag/2051 pix/yr [ii] % flux loss (in 2020)

Table 2: CTE residual flux loss evolution and percent flux loss results for four background levels in short and long exposure images using the new 2021 v2.0 `flc` data. All of the CTE flux loss percentages listed are for sources furthest from the readout amplifiers (maximum number of transfers) in the 2020 epoch. The CTE flux loss evolution for the 0.1-0.5 and 1-2 e$^-$ background has a baseline of 11 years (2009-2020). The CTE flux loss evolution for data with a 7-9 e$^-$ background level has a baseline of 8 years (2012-2020) and the baseline for the 12-12.5 e$^-$ background is 4 years (2016-2020). The units for each column are noted with the *i* and *ii* superscripts and listed under the table.

Table 3: CTE Flux Loss Evolution and Percent Flux Loss for New v2.0 `FLC` Data

Background [e$^-$]	13-15		19-21		25-27		34-36	
Flux Bin [e$^-$]	CTE loss rate^i	CTE flux loss^{ii}	CTE loss rate^i	CTE flux loss^{ii}	CTE loss rate^i	CTE flux loss^{ii}	CTE loss rate^i	CTE flux loss^{ii}
500-2000	0.01	12%	0.01	10%	0.01	8%	0.006	6%
2000-8000	0.003	4%	0.001	3%	-4e-4	2%	0.001	0.8%
8000-32000	0.001	0.4%	-0.001	0.2%	-0.002	-0.1%	0.0008	-0.4%

[i] Δmag/2051 pix/yr [ii] % flux loss (in 2020)

Table 3: CTE residual flux loss evolution and percent flux loss results for four background levels in long exposure images using the new 2021 v2.0 `flc` data. All of the CTE flux loss percentages listed are for sources furthest from the readout amplifiers (maximum number of transfers) in the 2020 epoch. The CTE flux loss evolution for data with a 13-15 and 34-36 e$^-$ background level has a baseline of 8 years (2012-2020). The CTE flux loss evolution for the 19-21 and 25-27 e$^-$ background data has a baseline of 4 years (2016-2020). The units for each column are noted with the *i* and *ii* superscripts and listed under the table.

4 Conclusion

In this report we have analyzed the 2009-2020 external CTE data calibrated with `calwf3` version 3.6.0, which uses the new v2.0 pixel-based CTE-correction. After fitting the photometric correction model to the data we provide the derived (background specific) coefficients that can be used to further correct point-source photometry in v2.0 `flc.fits` images. We compared the CTE flux losses present in the old v1.0 CTE-correction (using `calwf3` version 3.5.0) to those in the new v2.0 correction for the 11 available background levels.

The main take-aways from this report are:

- The v1.0 CTE-correction model often over-corrects photometry. It works best at a background of ∼12 e^-, where sources with 250-500 e^- within a 3-pixel radius aperture furthest from the readout are over-corrected by ∼5% in 2020.
- The v2.0 CTE-correction model tends to under-correct photometry. This model works best at a background of ∼20 e^-, where sources with 250-500 e^- within a 3-pixel radius aperture furthest from the readout are under-corrected by ∼17% in 2020.
- The trade-offs between the two models are more pixel-based correction and noise amplification for v1.0, and less pixel-based correction for v2.0 but with significantly improved readnoise mitigation.
- As of April 2021, all UVIS `flc` and `drc` data products retrieved from MAST will be processed with the new v2.0 CTE-correction, first released in `calwf3 v3.6.0` and beyond.
- Users have the option of calibrating their data with the v1.0 model following the instructions in a Jupyter-Notebook that can be found on the WFC3 CTE resource page[5].

The under-correction in the v2.0 model is largely by design (Anderson et al. 2021). At backgrounds where the CTE losses are greater than 25%, it is not possible to correct sources without dramatically amplifying background noise. The correction therefore takes a more conservative approach and as a result almost never amplifies noise. The new model is mostly limited to addressing pixel-to-pixel variations larger than the background fluctuations. When the v2.0 algorithm tries to adjust a pixel with a value less than the calculated pixel-to-pixel noise in the background, the amount of correction applied is appreciably reduced (Anderson et al. 2021).

It is worth noting that although the CTE decline from 12+ years of sustained radiation damage has made it hard to reconstruct the faintest sources on low backgrounds far from the amplifier, there are ways such faint sources can still be measured successfully without unduly amplifying readnoise. The best strategy is to minimize losses in the first place, by placing the source near the amplifier (when possible) and post-flashing to ensure adequate total background. Finally, there is no added noise in the uncorrected images, so one can

[5]https://www.stsci.edu/hst/instrumentation/wfc3/performance/cte

measure the source on the `flt` images and correct the surviving counts directly for that loss. See Kuhn and Bajaj (2021) for photometric correction model coefficients to correct CTE flux losses in `flt` images.

Acknowledgements

The author thanks Sylvia Baggett for reviewing this ISR and for providing crucial guidance and leadership throughout the project. The author graciously recognizes Varun Bajaj for his help in getting the initial calibration and analysis operating correctly and efficiently. We would also like to acknowledge the WFC3 ISR Editor Joel Green for providing many useful comments and edits. Thank you to Michele De La Pena for providing test environments and assisting with the integration of the v2.0 CTE-correction into the `calwf3` pipeline.

References

Anderson, J. and L. Bedin (Sept. 2010). "An Empirical Pixel-Based Correction for Imperfect CTE. I. HST's Advanced Camera for Surveys". In: 122.895, p. 1035. DOI: 10.1086/656399. arXiv: 1007.3987 [astro-ph.IM].

Anderson et al., J. (June 2021). *Updating the WFC3/UVIS CTE Model and Mitigation Strategies*. Instrument Science Report WFC3 2021-in prep.

Baggett, S. et al. (Jan. 2011). *Charge transfer efficiency (CTE) in the WFC3/UVIS CCDs*. WFC3 Whitepaper. https://www.stsci.edu/files/live/sites/www/files/home/hst/instrumentation/wfc3/performance/cte/_documents/cte.pdf.

Kozhurina-Platais et al. (Feb. 2011). *WFC3/UVIS-Cycle17: CTE External Monitoring - NGC6791*. Instrument Science Report WFC3 2011-06.

Kuhn, B. and V. Bajaj (Feb. 2021). *WFC3/UVIS External CTE Monitoring 2009-2020*. Instrument Science Report WFC3 2021-03.

Noeske, K. et al. (June 2012). *WFC3 UVIS Charge Transfer Eciency October 2009 to October 2011*. Instrument Science Report WFC3 2012-09.

Appendix

Empirical Photometric Correction Model

As presented in Noeske et al. (2012), the bivariate polynomial used to estimate CTE-induced flux loss is defined in terms of S:

$$S = \sum_{i,j=0}^{2} c_{ij} d^i f^j \tag{1}$$

where c_{ij} are the polynomial coefficients, f is the log_{10}(Flux) of the source, and the observation date is $d = MJD - 55400$. Expanding equation 1 then gives:

$$S = c_{00} + c_{01}f + c_{02}f^2 + d(c_{10} + c_{11}f + c_{12}f^2) + d^2(c_{20} + c_{21}f + c_{22}f^2) \tag{2}$$

Using the coefficients provided below in Tables 4 - 6 and solving for S in Equation 2, observers can estimate the CTE-corrected magnitude of their point-source photometry with:

$$m_{corr} = m_0 - S\frac{Y}{2051} \tag{3}$$

where m_0 is the uncorrected magnitude, and Y is the number of detector rows the source is away from the amplifier. The coefficients chosen for the model should be those corresponding to conditions that best match the observations attempting to be corrected. Additionally, **the coefficients below should only be used to correct photometry in UVIS `flc.fits` files corrected with the v2.0 pixel-based CTE correction, which was first released in `calwf3 3.6.0`**. Readers interested in coefficients for UVIS `flt.fits` or v1.0 `flc.fits` images should see Kuhn and Bajaj (2021) or the text files available on the WFC3 CTE resource page[6].

[6]https://www.stsci.edu/hst/instrumentation/wfc3/performance/cte

Table 4: Empirical CTE model coefficients for new 2021 CTE-corrected `FLC` data

Filter, Exposure Time Background [e^-]	F502N, Short $\sim$ 0.1-0.5	F502N, Short $\sim$ 12-12.5	F502N, Long $\sim$ 1-3	F502N, Long $\sim$ 13-15
C_{00}	4.39e-01	-1.74e-01	8.51e-01	2.61e-02
C_{01}	-1.48e-01	4.81e-02	-4.06e-01	-1.45e-02
C_{02}	1.18e-02	2.88e-03	4.76e-02	3.25e-04
C_{10}	1.95e-03	9.16e-04	4.27e-04	4.52e-04
C_{11}	-9.58e-04	-4.27e-04	-1.57e-04	-1.94e-04
C_{12}	1.15e-04	4.60e-05	1.43e-05	2.21e-05
C_{20}	-3.27e-07	-1.47e-07	-1.65e-07	-2.50e-08
C_{21}	1.53e-07	7.42e-08	6.78e-08	8.04e-09
C_{22}	-1.71e-08	-8.60e-09	-7.00e-09	-7.93e-10

Table 2: The polynomial coefficients for the empirical CTE-correction model using the new 2021 CTE-corrected `flc` data. The four F502N observing modes listed are a combination of long and short exposure images with both 0 and 12 e^-/pixel post-flash ($\sim$0.1 - 15 e^- background).

Table 5: Empirical CTE model coefficients for new 2021 CTE-corrected `FLC` data

Filter, Exposure Time Background [e^-]	F502N, Long $\sim$ 7-9	F502N, Long $\sim$ 19-21	F502N, Long $\sim$ 25-27	F502N, Long $\sim$ 34-36
C_{00}	-8.00e-02	1.44e+00	-1.68e-01	3.54e-01
C_{01}	6.06e-02	-6.72e-01	1.28e-01	-1.79e-01
C_{02}	-1.15e-02	8.27e-02	-1.53e-02	2.09e-02
C_{10}	9.51e-04	-6.52e-04	4.85e-04	-7.25e-05
C_{11}	-4.54e-04	3.06e-04	-2.68e-04	4.78e-05
C_{12}	5.58e-05	-3.86e-05	3.23e-05	-6.03e-06
C_{20}	-1.26e-07	1.69e-07	-4.79e-08	6.62e-08
C_{21}	6.17e-08	-7.90e-08	3.02e-08	-3.58e-08
C_{22}	-7.84e-09	9.69e-09	-3.81e-09	4.53e-09

Table 3: The polynomial coefficients for the empirical CTE correction model using the new 2021 CTE-corrected `flc` data. The four F502N observing modes listed are long exposure images with a $\sim$6 - 33 e^-/pixel post-flash (7 - 36 e^- background).

Table 6: Empirical CTE model coefficients for new 2021 CTE-corrected `FLC` data

Filter, Exptime Background [e^-]	F502N, Long $\sim$ 56-58	F502N, Long $\sim$ 92-94	F502N, Long $\sim$ 117-119
C_{00}	-1.41e-01	-2.96e-01	-9.47e-03
C_{01}	7.37e-02	1.35e-01	-5.61e-03
C_{02}	-1.15e-02	-1.78e-02	7.63e-05
C_{10}	3.46e-04	3.53e-04	-9.54e-05
C_{11}	-1.79e-04	-1.73e-04	3.87e-05
C_{12}	2.45e-05	2.30e-05	-2.84e-06
C_{20}	-2.72e-08	-4.66e-08	4.22e-08
C_{21}	1.41e-08	1.99e-08	-2.26e-08
C_{22}	-2.14e-09	-2.50e-09	2.79e-09

Table 4: The polynomial coefficients for the empirical CTE correction model using the new 2021 CTE-corrected `flc` data. The three F502N observing modes listed are long exposure images with a 55 - 116 e^-/pixel post-flash ($\sim$56 - 119 e^- background).